Self-force calculations for Kerr black hole inspirals

A Review of Recent Progress

Sam Dolan

University of Southampton

@ IST, Lisbon, Jan 2012

Talk Overview

1. Introduction to Gravitational Self-Force
    - Motivations
    - Key ideas
    - Calculation methods
2. Recent Progress
    - Gauge-invariant* comparisons with PN, NR & EOB
    - First self-forced evolutions
    - Resonances in EMRIs
3. The frontier: Kerr spacetime
    - The m-mode regularization method
    - Non-radiative modes & linearly-growing gauge modes
    - Latest results
4. Conclusion

Motivation I: EMRIs

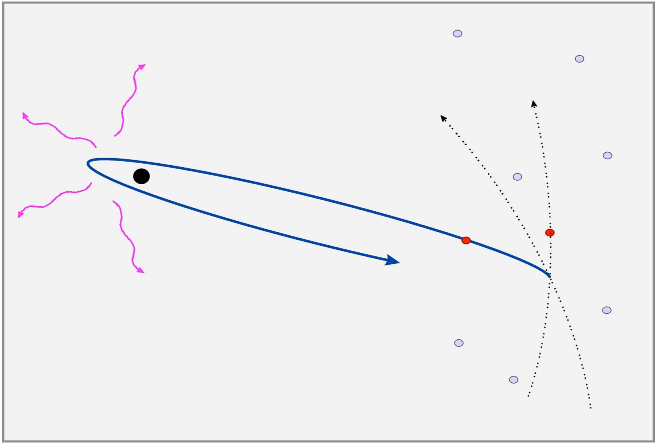

Motivation I: EMRIs

- A typical galaxy contains:
  1. A massive central BH (M)
  2. A population of compact objects (μ) within cusp ($r_{\text{cusp}} \sim 1\text{pc}$).
- Extreme mass-ratio $q = \mu/M = 10^{-5} — 10^{-8}$
- Two-body scattering of objects into nearly-parabolic orbits
- Highly eccentric $1 - e \sim 10^{-6} - 10^{-3}$, $p \sim 8 - 100M$
- Inspiral and capture if $t_{gw} \leq (1 - e)t_{relax}$
- Radiation reaction reduces eccentricity, but ...
- ... inspiral orbits are still typically:
  1. moderately eccentric even up to plunge
  2. non-equatorial (not aligned with BH spin)

Motivation II: LISA?

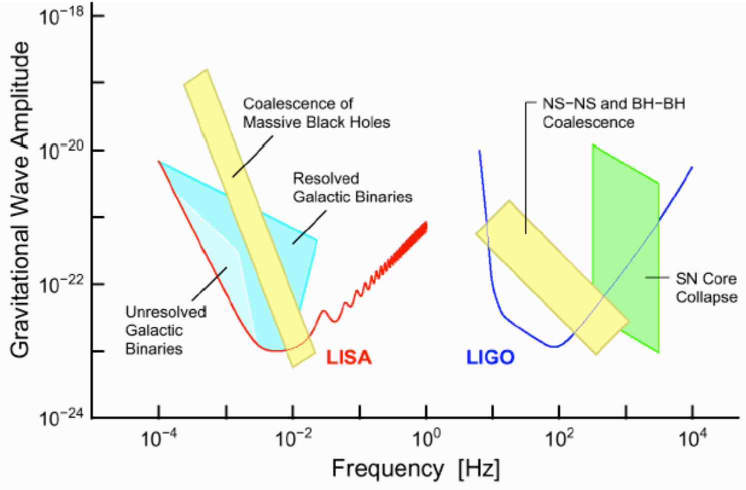

Motivation II: re-scoped LISA!

> "The new [LISA] configuration should detect thousands of galactic binaries, tens of (super)massive black hole mergers out to a redshift of z=10 and tens of extreme mass ratio inspirals out to a redshift of 1.5 during its two year mission."

Karsten Danzmann, Aug 2011.

Motivation III: the general 2-body problem in relativity

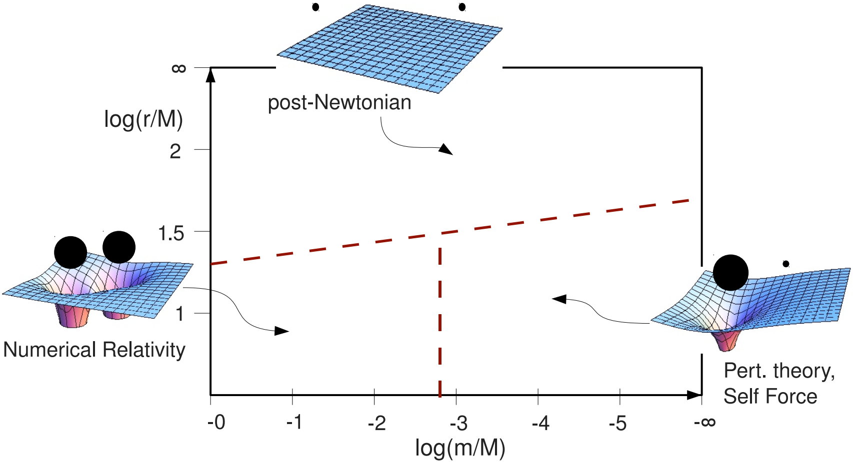

Motivation III: the general 2-body problem in relativity

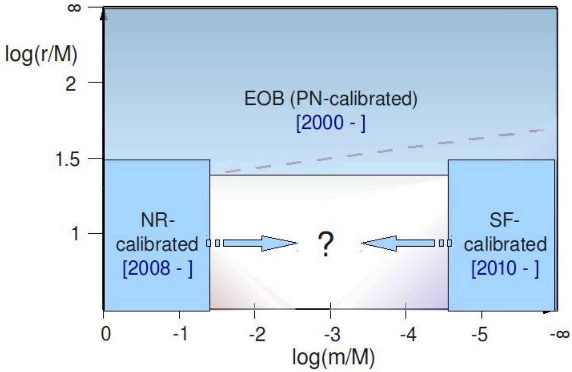

- Effective One-Body (EOB) formulation of Damour *et al.* provides a possible analytic fitting framework

Ideas I: Radiation Reaction in Electromagnetism

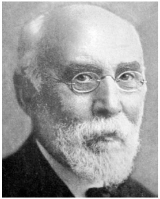

- An accelerated charge emits radiation
- Loss of energy $\Rightarrow$ force acting on charge
- Interpretation: the accelerated charge interacts with its own field
- Point charge $\Leftrightarrow$ infinite field ... mathematical problems?
- A regularization method is needed.

Ideas I: Radiation Reaction in Electromagnetism

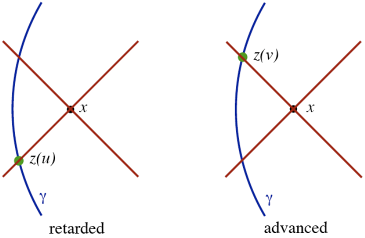

- Dirac split the electromagnetic potential A^μ into 'S' and 'R' parts:

$$
\begin{aligned}
A_S^\mu &= \frac{1}{2}\left(A_{\rm ret}^\mu + A_{\rm adv}^\mu\right) \\
A_R^\mu &= \frac{1}{2}\left(A_{\rm ret}^\mu - A_{\rm adv}^\mu\right)
\end{aligned}
$$

- 'S' for symmetric / singular
- 'R' for radiative / regular
- Self-Force from $F_\mu = \nabla^\nu F^R_{\mu\nu}$, where $F^R_{\mu\nu} = \nabla_\mu A^R_\nu - \nabla_\nu A^R_\mu$

Ideas II: Self-Force in Curved Spacetime

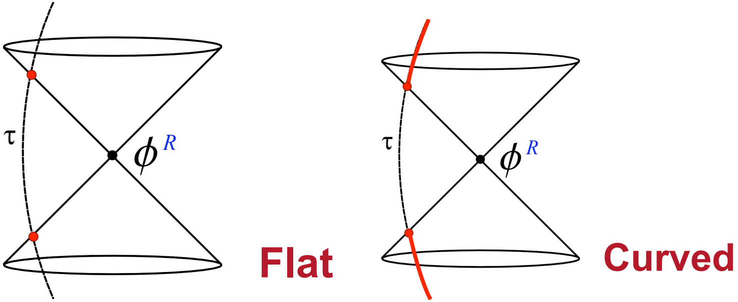

- In flat spacetime, Green function has support on light-cone only.
- In curved spacetime, Green function also has a ‘tail’ within the light cone.
- Also, the light cone intersects itself (light ring at $r = 3M$)
- Dirac’s radiative potential becomes non-causal in curved spacetimes.

(Intersecting Light Cone)

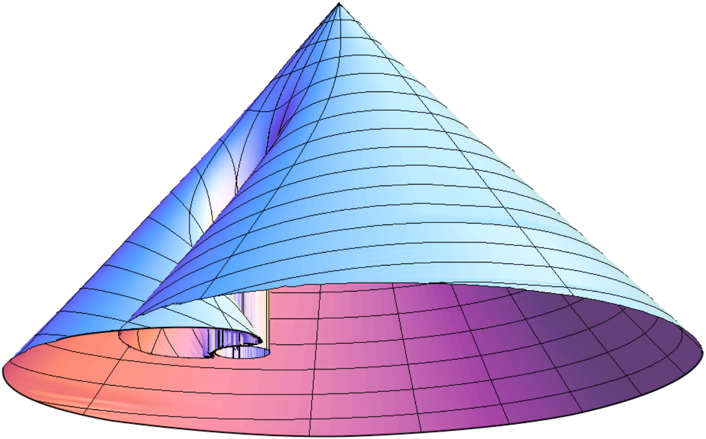

See e.g. V. Perlick's Living Review on lensing.

Ideas II: SF in Curved Spacetime: Electromagnetism

- DeWitt & Brehme (1960) derived the EM SF in curved spacetime

$$
\begin{aligned}
ma^\mu &= f^\mu_{\text{ext}} + e^2 \left(\delta^\mu_\nu + u^\mu u_\nu\right) \left(\frac{2}{3m} \frac{df_{\text{ext}}}{d\tau} + \frac{1}{3} R^\nu{}_\lambda u^\lambda \right) \\
&\quad + 2e^2 u_\nu \lim_{\epsilon \rightarrow 0} \int_{-\infty}^{\tau - \epsilon} \nabla^{[\mu} G^{\nu]}_{\text{ret}\,\lambda} \left(z(\tau), z(\tau')\right) u^\lambda d\tau'
\end{aligned}
$$

- Tail integral over past history of motion is v. difficult to compute!
- Need practical regularization schemes that avoid tail integral in this form

Ideas II: SF in Curved Spacetime: Gravitational

- Charge $e \to$ mass μ, field $A_\mu \to$ metric perturbation $h_{\mu\nu}$
- Equations for (first-order in μ) 'Gravitational Self-Force' (GSF)
- Formally derived via Method of Matched Asymptotic Expansions
- Obtained by Mino, Sasaki & Tanaka, and Quinn & Wald (1997).
- Known as the MiSaTaQuWa equation
- MiSaTaQuWa equation still features a tail integral
- Need regularization schemes for practical calculations.

Ideas II: Regularization Method

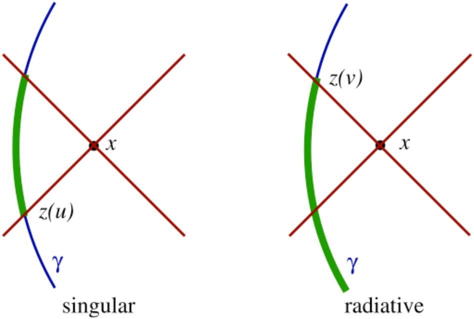

- Dirac's split into R and S fields was acausal
- Alternative Detweiler-Whiting split (2003) into $\tilde{S}$ and $\tilde{R}$ fields is causal
- Correct 'MiSaTaQuWa' self-force is recovered from $\tilde{R}$ part.
- $\tilde{S}$ part not known exactly (global existence questionable), but it can be computed in vicinity of worldline via series expansions.

Ideas III: Dissipative/Conservative Parts of Self-Force

- Scalar field example: Retarded and advanced fields Φ_{ret} and Φ_{adv}
- Ret. and adv. 'R' fields, $\Phi^R_{\text{ret}} = \Phi_{\text{ret}} - \Phi_S$, $\Phi^R_{\text{adv}} = \Phi_{\text{adv}} - \Phi_S$
- Define conservative and dissipative parts of field

$$\begin{aligned} \Phi^{\text{cons}} &= \frac{1}{2}\left(\Phi^R_{\text{ret}} + \Phi^R_{\text{adv}}\right) = \frac{1}{2}\left(\Phi_{\text{ret}} + \Phi_{\text{adv}} - 2\Phi_S\right) \\ \Phi^{\text{diss}} &= \frac{1}{2}\left(\Phi^R_{\text{ret}} - \Phi^R_{\text{adv}}\right) = \frac{1}{2}\left(\Phi_{\text{ret}} - \Phi_{\text{adv}}\right) \end{aligned}$$

- Dissipative part does not need regularization!
- Conservative part needs knowledge of S field.
- Dissipative part $\Rightarrow$ secular loss of energy and angular momentum.
- Conservative part $\Rightarrow$ shift in orbital parameters, periodic.

Ideas IV: Interpretation of Gravitational Self-Force

accelerated motion on a background spacetime

$$\mu \vec{a}_g = \vec{F}_{\mathrm{self}} = \vec{F}_{\mathrm{diss}} + \vec{F}_{\mathrm{cons}}$$

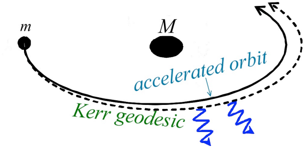

$$\Updownarrow$$

geodesic motion in a perturbed spacetime

$$\mu \vec{a}_{g+h} = 0$$

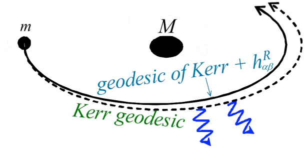

Methods I: ℓ-mode regularization

Define $F^{\alpha}_{\mathrm{ret}/S} \equiv \mu k^{\alpha\mu\nu\beta} \nabla_{\beta} \bar{h}^{\mathrm{ret}/S}_{\mu\nu}$ (as fields), then write

$$
\begin{aligned}
F_{\mathrm{self}} &= \left. (F_{\mathrm{ret}} - F_{\mathrm{S}}) \right|_{\mathrm{p}} \\
&= \sum_{\ell=0}^{\infty} \left. \left(F^{\ell}_{\mathrm{ret}} - F^{\ell}_{S} \right) \right|_{\mathrm{p}} \qquad (\ell\text{-mode contributions are finite}) \\
&= \sum_{\ell=0}^{\infty} \left[F^{\ell}_{\mathrm{ret}}(p) - AL - B - C/L \right] - \sum_{\ell=0}^{\infty} \left[F^{\ell}_{S}(p) - AL - B - C/L \right] \\
&= \sum_{\ell=0}^{\infty} \left[F^{\ell}_{\mathrm{ret}}(p) - AL - B - C/L \right] - D \qquad (\text{where } L = \ell + 1/2)
\end{aligned}
$$

- Regularization Parameters A, B, C, D calculated analytically for generic orbits in Kerr in Lorenz gauge $\bar{h}^{;\nu}_{\mu\nu} = 0$.
- Works well for spherically-symmetric spacetimes (e.g. Schw.) which allow decomposition in tensor spherical harmonics

Methods II: Puncture Schemes

- Metric perturbation $g_{\mu\nu}^{\text{Schw/Kerr}} + h_{\mu\nu}$
- Trace-reversed MP: $\bar{h}_{\mu\nu} = h_{\mu\nu} - \frac{1}{2} g_{\mu\nu} h$
- Work in Lorenz gauge $\bar{h}_{\mu\nu}^{;\nu} = 0$. Four gauge constraints.
- 10 wave equations: (neglecting $(\mu/M)^2$ and higher)

$$\Box \bar{h}_{\mu\nu} + 2 R^{\alpha}{}_{\mu}{}^{\beta}{}_{\nu} \bar{h}_{\alpha\beta} = -16\pi T_{\mu\nu}$$

- Delta-function source,

$$T_{\mu\nu}(x^{\alpha}) = \mu \int_{-\infty}^{\infty} (-g)^{-1/2} \delta^4[x^{\alpha} - x_p^{\alpha}(\tau)] u_{\mu} u_{\nu} d\tau.$$

- In 1+1D, MP is C^0 on the worldline. In 2+1D, MP diverges logarithmically. In 3+1D, diverges as 1/distance.
- Idea: evolve a 'residual field' $h^{\text{res}} = h^{\text{ret}} - h^{\text{punc}}$, where h^{punc} is some local approximation to $h^{\tilde{S}}$.

A (selective) review of progress since 2009

1. First comparison of gauge-invariant results with Post-Newtonian theory (PN) and Numerical Relativity (NR):
   - ISCO shift due to conservative part of GSF
   - Perihelion advance of eccentric orbits
   - Benefits of using 'symmetric mass-ratio'
2. Calibration of Effective One-Body (EOB) theory with GSF
3. First 'self-forced' evolutions:
   1. via method of osculating geodesics
   2. with time domain code (scalar-field)
4. Resonances in EMRIs on Kerr spacetime

1. Comparisons: (I) The redshift invariant

- Circular geodesic motion on Schwarzschild at radius $r > 3M$,

$$E = \frac{r-2M}{\sqrt{r(r-3M)}}\mu, \qquad \frac{dE}{dt} = -F_t/u_0^t$$

- The dissipative components, F_t and F_r, corresponding to energy and angular momentum loss, are gauge-invariant(*).
- The conservative component F_r is gauge-dependent.
- Detweiler identified two quantities which are gauge invariant under transforms that respect the helical symmetry of the circular orbit.
  1. Orbital frequency $\Omega \Leftrightarrow$ radius $R \equiv (M/\Omega^2)^{1/3}$
  2. Redshift $z = 1/u^t$
- Both defined w.r.t Schw. t coordinate of background spacetime.
- $z(R)$ is a gauge-invariant relation.
- Independent results of Regge-Wheeler and Lorenz gauge calculations compared by Detweiler, and Sago & Barack (2008).

1. Comparisons: (II) The ISCO shift

- Innermost stable circular orbit (ISCO) where $dE/dr = 0$.
- For geodesic motion,

$$r_{\text{isco}} = 6M, \qquad \Omega_{\text{isco}} = \left(6^{3/2}M\right)^{-1}.$$

- The conservative part of GSF shifts the ISCO by $O(\mu)$.
- $\Delta\Omega_{\text{isco}}$ is invariant under gauge transformations that respect the helical symmetry of the circular orbit.
- GSF prediction:

$$\boxed{\frac{\Delta\Omega_{\text{isco}}}{\Omega_{\text{isco}}} = 0.4870\mu/M}$$

- Barack & Sago, PRL **102**, 191101 (2009), arXiv:0902.0573.

1. Comparisons: (II) The ISCO shift

- GSF prediction must be modified for comparison with PN, because Lorenz gauge is not asymptotically-flat ($h_{tt} \sim \mathcal{O}(r^0)$).
- Apply simple monopolar gauge transformation to get:

$$\boxed{\frac{\Delta\Omega_{\rm isco}}{\Omega_{\rm isco}} = 1.2512\,\mu/M}$$

- A challenge: can a resummed Post-Newtonian expansion match this strong-field result?
- Challenge taken up in M. Favata, PRD **83**, 024027 (2011), arXiv:1008.4622.

1. Comparisons: (II) The ISCO shift

Method	$c_\Omega^{\rm PN}$	Δ_{c_Ω}
A4PN-P$_A$	1.132	−0.0955
A4PN-T$_A$	1.132	−0.0955
$C_0$3PN	1.435	0.1467
e2PN-P	1.036	−0.1717
KWW-1PN	1.592	0.2726
A3PN-P	0.9067	−0.2754
A3PN-T	0.9067	−0.2754
A4PN-P$_B$	0.8419	−0.3272
A4PN-T$_B$	0.8419	−0.3272
j3PN-P	1.711	0.3671
j2PN-P	0.6146	−0.5088
KWW-S	0.5610	−0.5515
$C_0$2PN	0.5833	−0.5338
E_h3PN	0.4705	−0.6240
e3PN-P	2.178	0.7409
A2PN-P	0.2794	−0.7767
A2PN-T	0.2794	−0.7767
E_h2PN	0.0902	−0.9279
E_h1PN	−0.014 73	−1.011
E_h-S	−0.054 71	−1.044
HH-S	−0.1486	−1.119
j1PN-P	−0.1667	−1.133
KWW-2PN	−1.542	−2.232
j-P-S	−2.104	−2.682
KWW-3PN	4.851	2.877
HH-1PN	6.062	3.844
HH-2PN	−12.75	−11.19
HH-3PN	25.42	19.32

- Table 1 in M. Favata, PRD **83**, 024027 (2011), arXiv:1008.4622.

1. Comparisons: (III) The periastron advance

- GR $\Rightarrow$ periastron advance $\delta = \frac{6\pi M}{[(1-e^2)p]}$ (e.g. 43" per century for Mercury).
- Conservative part of GSF $\Rightarrow \Delta\delta \sim O(\mu)$
- $\Delta\delta < 0$ for all eccentric orbits
- $\Delta\delta$ is gauge-invariant (within restricted class of gauges) …
- …but its parameterization $\Delta\delta(p, e)$ is not.
- Numerical results in Barack & Sago, PRD **83**, 084023 (2011), arXiv:1101.3331.

1. Comparisons: (III) The periastron advance

- Periastron advance was recently compared between NR, PN, EOB and GSF in comparable mass regime $1/8 \leq \mu/M \leq 1$.
- Le Tiec *et al.* PRL **107**, 141101 (2011) [arXiv:1106.3278]
- Remarkably, the GSF prediction works well even in comparable mass regime if we replace μ/M with symmetric mass ratio:

$$\mu/M \rightarrow \mu M/(\mu + M)^2$$

- Plots on next slide show $K = \Omega_\phi/\Omega_r = 1 + \delta/(2\pi)$.

1. Comparisons: (III) The periastron advance

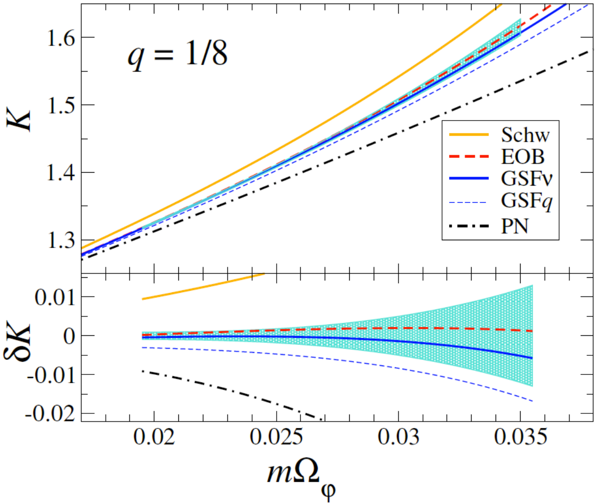

From Le Tiec, Mroué, Barack, Buonanno, Pfeiffer, Sago and Taracchini, PRL **107**, 141101 (2011), arXiv:1106.3278.

1. Comparisons: (III) The periastron advance

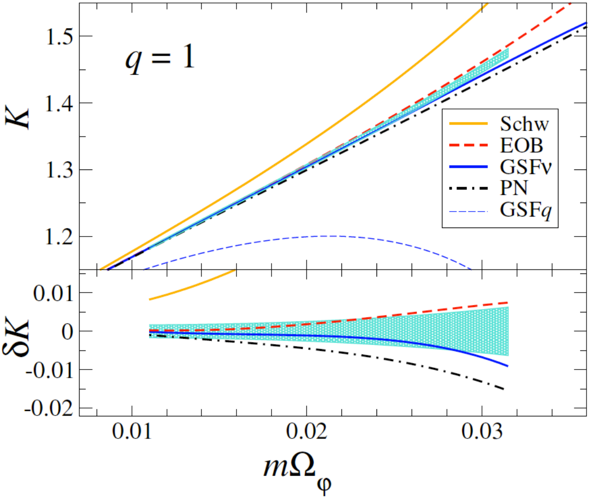

From Le Tiec, Mroué, Barack, Buonanno, Pfeiffer, Sago and Taracchini, PRL **107**, 141101 (2011), arXiv:1106.3278.

2. Calibration of Effective One-Body theory

- Damour and collaborators have fed GSF results into the EOB model.
- Idea: Compare precession of small-eccentricity orbits at first-order in μ

$$\frac{\Omega_r^2}{\Omega_\phi^2} = 1 - 6x + \left(\frac{\mu}{M}\right) \rho(x) + O\left((\mu/M)^2\right)$$

where

$$x \equiv \left[(M+\mu)\Omega_\phi\right]^{2/3}.$$

- PN theory gives the (weak-field) expansion

$$\rho^{PN}(x) = \rho_2 x^2 + \rho_3 x^3 + (\rho_4^c + \rho_4^{\log} \ln x) x^4 + (\rho_5^c + \rho_5^{\log} \ln x) x^5 + O(x^6)$$

- ρ_2, ρ_3 are given by 3PN.
- logarithmic contributions at 4PN and 5PN ($\rho_4^{\log}$ and $\rho_5^{\log}$) have been derived by Damour
- ρ_4^c and ρ_5^c are (presently) unknown in PN.

2. Calibration of Effective One-Body theory

- Using accurate GSF results, $\{\rho_2, \rho_3, \rho_4^{\log}, \rho_5^{\log}\}$ may be tested, and the unknown parameters ρ_4^c and ρ_5^c may be constrained:

$$\boxed{\rho_4^c = 69^{+7}_{-4}, \qquad \rho_5^c = -4800^{+400}_{-1200}, \qquad \rho_6^{\log} < 0.}$$

- Determination of $\rho(x)$ in the range $0 \leq x \leq 1/6$ gives first info on strong-field behaviour of a combination of EOB functions $a(u)$ and $d(u)$ [where $u = G(M+\mu)/(c^2 r_{EOB})$].
- Advantage of GSF calibration: Both GSF and EOB split naturally into conservative and dissipative effects.
- GSF data for $\rho(x)$ may be fitted with simple 2-point Pade approximation that also makes use of PN information.

2. Calibration of EOB model

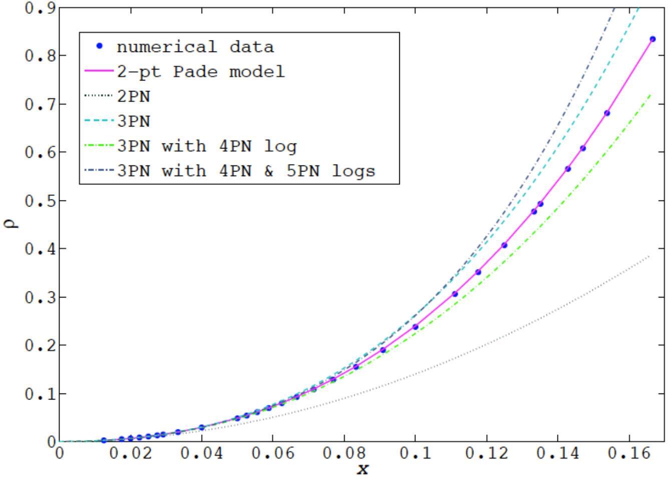

From Barack, Damour and Sago, Phys. Rev. D **82**, 084036 (2010) [arXiv:1008.0935].

3. Self-forced evolutions

- Want to evolve self-forced orbits over 10^5 cycles!
- Pound & Poisson [PRD**77**, 044013 (2008)] described a method of osculating geodesics for self-forced evolutions.
- Requires a fit to GSF data over a range of (p, e) with analytic model.
- First evolutions recently performed by Warburton, Akcay, Barack, Gair & Sago [arXiv:1111.6908].
- Animations follow, showing two simulations: (i) with full GSF; (ii) with only dissipative part of GSF.

- Rather than computing GSF w.r.t. geodesics of background, the aim is to evolve self-consistently in the time domain.
- Diener, Vega, Wardell and Detweiler [arXiv:1112.4821] have looked at scalar-field case:

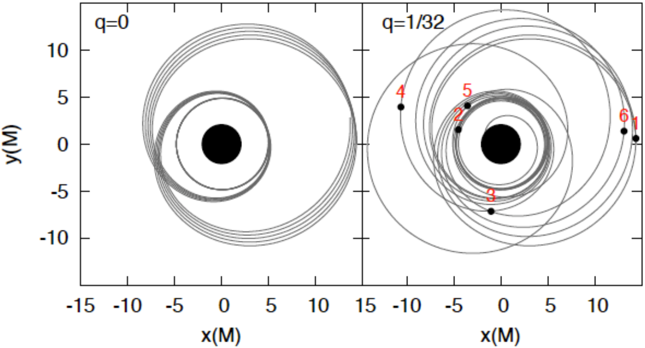

4. Resonances (I)

- Two timescales: (i) orbital period $\sim M$, (ii) radiation reaction μ^{-1}.
- Hinderer & Flanagan (2010) describe two-timescale expansion for EMRIs, using action-angle variables.
- Action : 'constants' of motion : $J_\nu = \left(E/\mu, L_z/\mu, Q/\mu^2\right)$
- Angle : 'phase' variables $q_\alpha = (q_t, q_r, q_\theta, q_\phi)$.
- $q_r \rightarrow q_r + 2\pi$ as orbit goes $r = r_{\text{min}} \rightarrow r_{\text{max}} \rightarrow r_{\text{min}}$ with period $\tau_r = 2\pi/\omega_r$.
- Frequencies $\omega_\alpha(J) = (\omega_r, \omega_\theta, \omega_\phi)$
- Generic geodesic orbits on Kerr are ergodic (space-filling).
- Isometries of Kerr $\Rightarrow$ (q_t, q_ϕ) 'irrelevant', (q_r, q_θ) 'relevant' params.

4. Resonances (II)

1. Geodesic approximation ($\eta = 0$):

$$\frac{dq_\alpha}{d\tau} = \omega_\alpha(J)$$
$$\frac{dJ_\nu}{d\tau} = 0$$

Solution :

$$q_\alpha(\tau, \eta = 0) = \omega_\alpha \, \tau \quad (1)$$
$$J_\nu(\tau, \eta = 0) = \text{const.} \quad (2)$$

Timescale : unchanging

2. Adiabatic approximation:

$$\begin{aligned} \frac{dq_\alpha}{d\tau} &= \omega_\alpha(J) \\ \frac{dJ_\nu}{d\tau} &= \eta \left\langle G_\nu^{(1)}(q_r, q_\theta, J) \right\rangle_{\text{orbital average}} \end{aligned}$$

Solution :

$$\begin{aligned} q_\alpha(\tau, \eta) &= \eta^{-1} \hat{q}(\eta\tau) \\ J_\nu(\tau, \eta) &= \hat{J}(\eta\tau) \end{aligned}$$

Timescale : $\tau_{rad.reac.} \sim \eta^{-1}$

4. Resonances (IV)

3. Post-adiabatic approximation:

$$\begin{aligned}
\frac{dq_\alpha}{d\tau} &= \omega_\alpha(J) + \eta g_\alpha^{(1)}(q_r, q_\theta, J) + \mathcal{O}(\eta^2) \\
\frac{dJ_\nu}{d\tau} &= \eta G_\nu^{(1)}(q_r, q_\theta, J) + \eta^2 G_\nu^{(2)}(q_r, q_\theta, J) + \mathcal{O}(\eta^3).
\end{aligned}$$

Two timescales : $\sim \eta^{-1}$ (secular) and ~ 1 (oscillatory).

4. Resonances (V)

Is adiabatic approximation justified? i.e. is it always OK to neglect fast-oscillating parts?

Consider Fourier decomposition

$$G_\nu^{(1)}(q_r, q_\theta, J) = \sum_{k_r, k_\theta} G^{(1)}_{\nu k_r, k_\theta}(J) e^{i(k_r q_r + k_\theta q_\theta)}$$

and $q_r = \omega_r \tau + \dot{\omega}_r \tau^2 + \ldots$, $q_\theta = \omega_\theta \tau + \dot{\omega}_\theta \tau^2 + \ldots$

$$k_r q_r + k_\theta q_\theta = \left(k_r \omega_r + k_\theta \omega_\theta\right) \tau + \left(k_r \dot{\omega}_r + k_\theta \dot{\omega}_\theta\right) \tau^2 + \ldots$$

Cannot neglect higher Fourier components if resonance condition

$$k_r \omega_r + k_\theta \omega_\theta = 0$$

is satisfied! i.e. when ω_r / ω_θ passes through low-order integer ratio.

4. Resonances (VI)

- Duration of resonance set by $(k_r \dot{\omega}_r + k_\theta \dot{\omega}_\theta)\, \tau^2 \sim 1$, i.e.

$$\tau_{\rm res} \sim 1/\sqrt{p\eta}$$

  where $p \equiv |k_r| + |k_\theta|, \quad \eta = \mu/M.$

- Net change in 'constants' of motion is

$$\Delta J \sim \sqrt{\eta/p}$$

- Net change in phase is

$$\Delta q \sim 1/\sqrt{\eta p}$$

- Need to know precise first-order SF and (possibly) dissipative part of 2nd-order SF to model resonance accurately.
- Without complete knowledge, a resonance effectively resets the phase and 'kicks' the orbital parameters.

4. Resonances (VII)

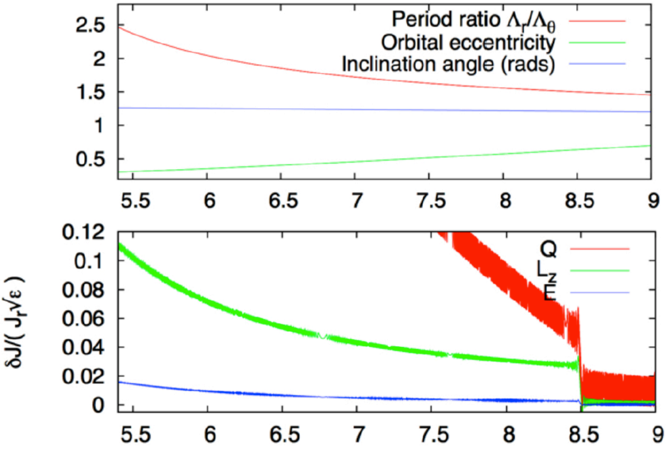

- Credit: Hinderer & Flanagan, arXiv:1009.4923.

GSF on Kerr: The frontier

- Schw. $\Rightarrow$ separability $\Rightarrow$ l-mode regularization $\Rightarrow$ easy!
  - decompose $\bar{h}_{ab}$ in tensor spherical harmonics $Y_{ab}^{lm(i)}$
  - use Lorenz gauge $\nabla^b \bar{h}_{ab} = 0$ with gauge constraint damping
  - solve 1+1D in time domain, or ODEs in freq. domain
  - apply l-mode regularization:

$$F_\mu^{\text{self}} = \sum_{\ell=0}^{\infty} \left[F_\mu^{\ell,\text{ret}} - A(l+1/2) - B - C/(l+1/2) \right] - D$$

GSF on Kerr: The frontier

- Kerr $\Rightarrow$ hard choices ... lack of separability ...
  - Teukolksy variables Ψ_0, Ψ_4 ...spin-weighted spheroidal harmonics ... metric reconstruction in radiation gauge (Chrzanowski) $\rightarrow$ Lorenz gauge? $l = 0, 1$ modes?
  - Hertz potential approach under development by Friedman *et al.*
  - tensor spheroidal harmonics ... [don't exist?]
  - Full 3+1D approach ... expensive!
  - m-mode + 2+1D evolution ... practical compromise.
- Proof-of-principle for m-mode recently established with scalar-field toy model for circular orbits on Kerr

$$\Phi_{\mathcal{R}} = \sum_{m=-\infty}^{\infty} \Phi_{\mathcal{R}}^{m} e^{im\varphi}, \quad F_r^m = q\partial_r \Phi_{\mathcal{R}}^m, \quad F_r = \sum_{m=-\infty}^{\infty} F_r^m$$

Puncture scheme : Scalar field implementation

- Local approximation Φ_P for Detweiler-Whiting S field Φ_S
- Covariant expansion $\rightarrow$ power series approximation in
  - coordinate differences $\delta x^a = x^a - \bar{x}^a$, where
  - x is field point, $\bar{x}$ is worldline point
- Classification: nth order expansion iff

$$\Phi_P^{[n]} - \Phi_S \sim \mathcal{O}(|\delta x| \delta x^{n-2})$$

- 4th-order expansions are available [arXiv:1107.0012, arXiv:1112.6355].
- From local expansion $\Phi_P^{[n]}$ to global puncture field $\Phi_{\mathcal{P}}^{[n]}$:
  - Let $\bar{x}$ become a function of x
  - e.g. set same BL time coordinate, $\bar{t} = t$
  - Periodic continuation: e.g. $\delta\varphi^2 \rightarrow 2(1 - \cos\delta\varphi) = \delta\varphi^2 + \mathcal{O}(\delta\varphi^4)$

Residual field + modal decomposition

- Introduce residual field: $\Phi_{\mathcal{R}}^{[n]} = \Phi - \Phi_{\mathcal{P}}^{[n]}$
- Residual field obeys wave equation,

$$\Box\Phi_{\mathcal{R}} = S_{\text{eff}}$$

  with effective source $S_{\text{eff}} = \int_\gamma \delta(x - \bar{x}(\tau))d\tau - \Box\Phi_{\mathcal{R}}^{n}$.
- Regularity: $S_{\text{eff}} \sim \mathcal{O}\left(|\delta x|\delta x^{n-4}\right)$

Residual field + modal decomposition

- Introduce residual field: $\Phi_{\mathcal{R}}^{[n]} = \Phi - \Phi_{\mathcal{P}}^{[n]}$
- Residual field obeys wave equation,

$$\Box \Phi_{\mathcal{R}} = S_{\text{eff}}$$

with effective source $S_{\text{eff}} = \int_\gamma \delta(x - \bar{x}(\tau)) d\tau - \Box \Phi_{\mathcal{R}}^{n}$.

- Regularity: $S_{\text{eff}} \sim \mathcal{O}\left(|\delta x| \delta x^{n-4}\right)$
- Decomposition in m modes:

$$\Phi_{\mathcal{R}} = \sum_{m=-\infty}^{\infty} \Phi_{\mathcal{R}}^{m} e^{im\varphi}, \quad \{\Phi_{\mathcal{P}}^{m}, S_{\text{eff}}^{m}\} = \frac{1}{2\pi} \int_{-\pi}^{\pi} \{\Phi_{\mathcal{P}}, S_{\text{eff}}\} \, e^{-im\varphi} d\varphi$$

- 2+1D wave equations:

$$\Box^{m} \Phi_{\mathcal{R}}^{m} = S_{\text{eff}}^{m}$$

Mode sums and convergence

- Field is real $\Rightarrow \Phi^{-m} = \Phi^{m*}$
- SF from mode sums, e.g.

$$F_r = q \sum_{m=0}^{\infty} \partial_r \tilde{\Phi}^m_{\mathcal{R}}$$

where

$$\tilde{\Phi}^m_{\mathcal{R}} = \begin{cases} \Phi^m_{\mathcal{R}}, & m = 0 \\ 2\,\mathrm{Re}\,\left(\Phi^m_{\mathcal{R}}\, e^{im\bar{\varphi}(t)}\right), & m \neq 0 \end{cases}$$

Mode sums and convergence

- Field is real $\Rightarrow \Phi^{-m} = \Phi^{m*}$
- SF from mode sums, e.g.

$$F_r = q \sum_{m=0}^{\infty} \partial_r \tilde{\Phi}_{\mathcal{R}}^{m}$$

where

$$\tilde{\Phi}_{\mathcal{R}}^{m} = \begin{cases} \Phi_{\mathcal{R}}^{m}, & m = 0 \\ 2\,\mathrm{Re}\left(\Phi_{\mathcal{R}}^{m}\, e^{im\bar{\varphi}(t)}\right), & m \neq 0 \end{cases}$$

- Power law convergence $F_r^m \sim m^{-\zeta}$ in large-m regime
- Convergence rate ζ depends on order n of puncture.
- $\zeta = n$ for n even, and $\zeta = n - 1$ for n odd.

Puncture order and m-mode convergence

For circular orbits, F_r is conservative and F_φ is dissipative.

punc. order	$\Phi_{\mathcal{R}}$	C	S_{eff}	Φ_R^m	F_r^m	F_φ^m
1	$\delta x / \lvert\delta x\rvert$	C^{-1}	$1/\delta x^2$	m^{-2}	—	—
2	$\lvert\delta x\rvert$	C^0	$1/\lvert\delta x\rvert$	m^{-2}	m^{-2}	$e^{-\lambda m}$
3	$\lvert\delta x\rvert \, \delta x$	C^1	$\delta x/\lvert\delta x\rvert$	m^{-4}	m^{-2}	$e^{-\lambda m}$
4	$\lvert\delta x\rvert \, \delta x^2$	C^2	$\lvert\delta x\rvert$	m^{-4}	m^{-4}	$e^{-\lambda m}$

World-tube construction

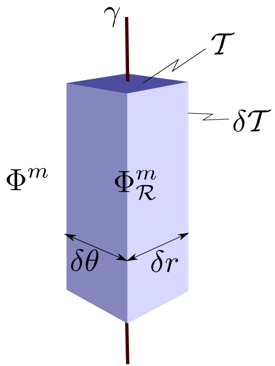

- Worldtube $\mathcal{T}$ of fixed dimensions δr, $\delta\theta$
- Outside: $\Box_m \Phi^m = 0$
- Inside: $\Box_m \Phi^m_{\mathcal{R}} = S^m_{\text{eff}}$
- Across boundary $\delta\mathcal{T}$: $\Phi^m_{\mathcal{R}} = \Phi^m - \Phi^m_{\mathcal{P}}$

Finite difference method in 2+1D

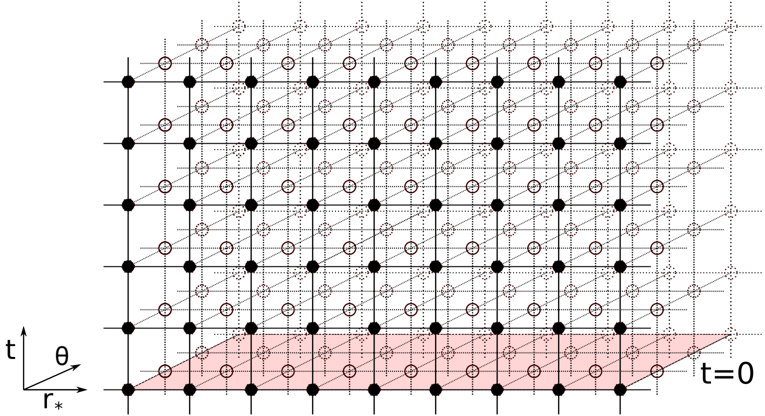

Spatial profile of modes: r_*

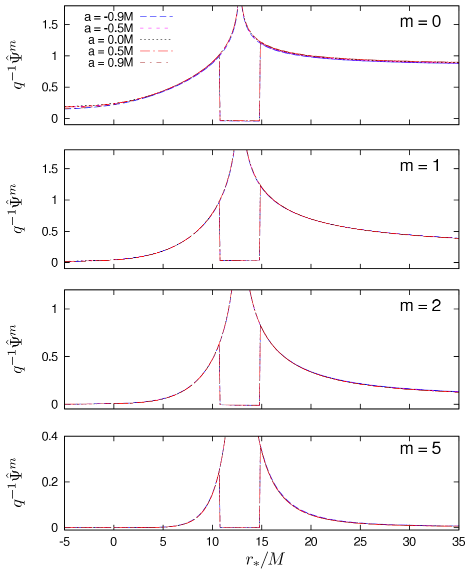

Spatial profile of modes: θ

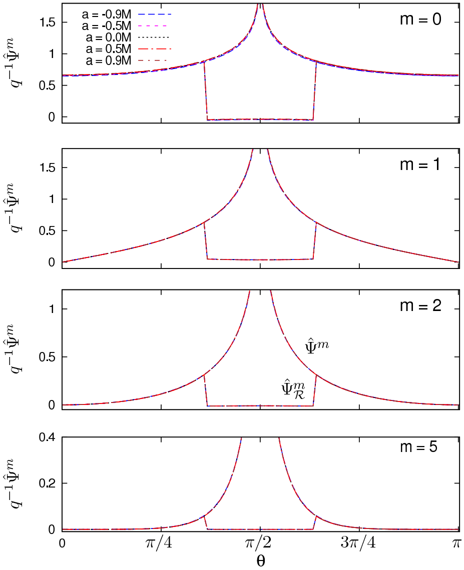

Spatial profiles: r_* and θ ($m = 0$)

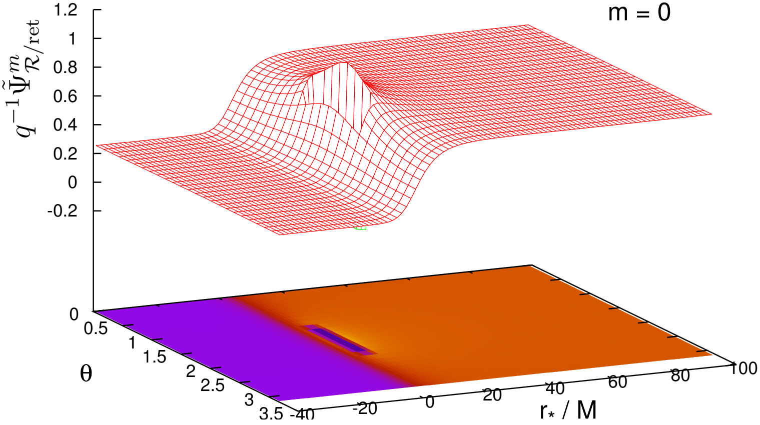

Spatial profiles: r_* and θ ($m = 1$)

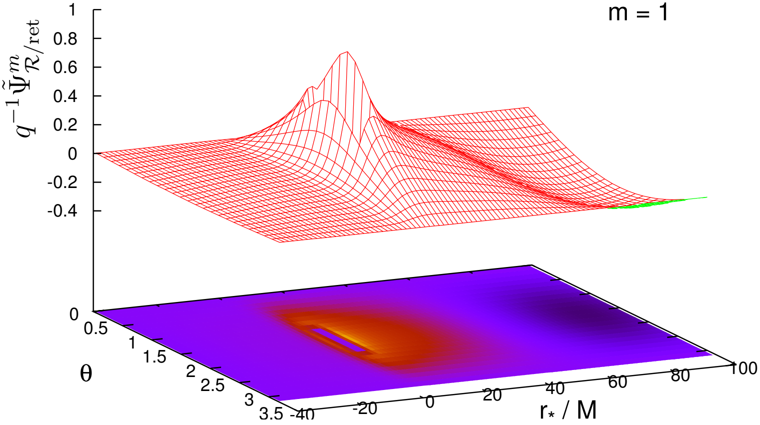

Spatial profiles: r_* and θ $(m = 5)$

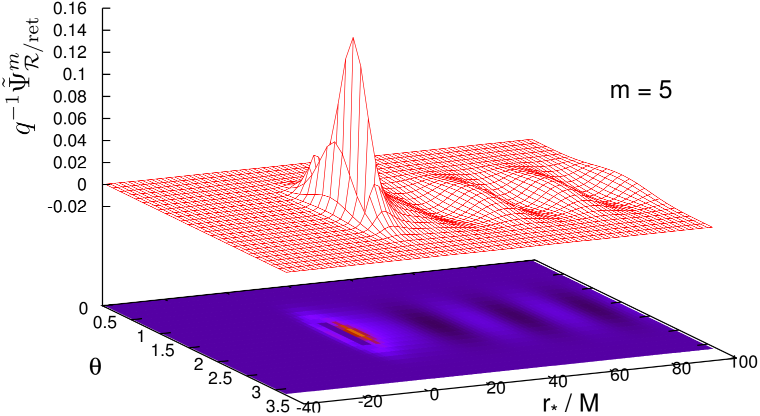

Spatial profiles: r_* and θ $(m = 10)$

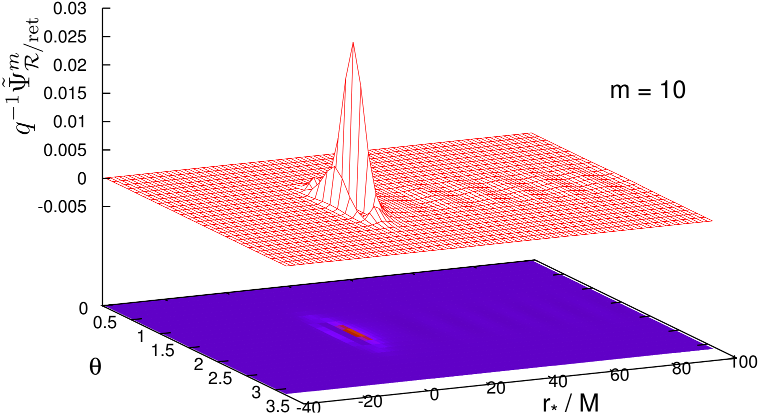

Time evolution of m-modes on worldline

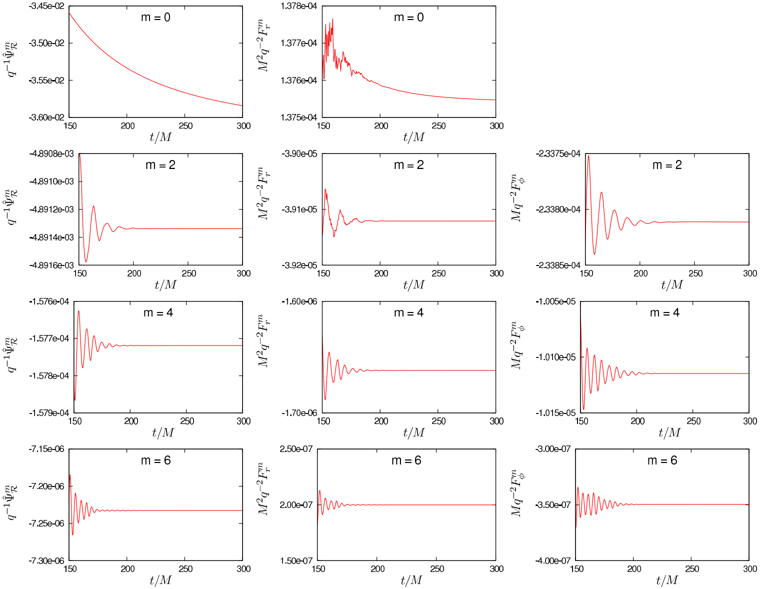

Low-m modes and power law relaxation

- Low-m modes take longest to relax
- Fit power-law decay model
- e.g. for $m = 0$, $\tilde{\Phi}^m_{\mathcal{R}}(t) = \tilde{\Phi}^m_{\mathcal{R}}(\infty) + c_2 t^{-\eta} + \ldots$

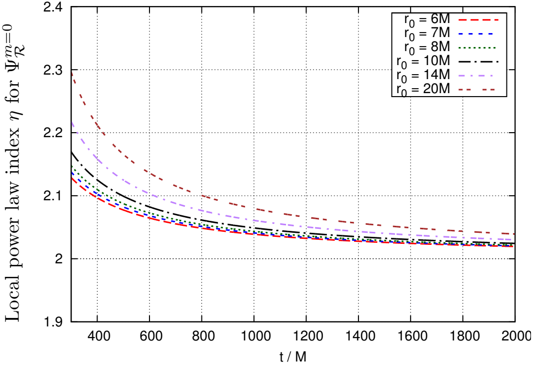

Richardson extrapolation (I)

Extrapolation to infinite resolution

- Results depends on grid resolution x, e.g. :

$$\triangle t = xM, \quad \triangle r_* = xM, \quad \triangle \theta = \pi x/6$$

- Second-order-accurate FD method $\Rightarrow$ error $\mathcal{O}(x^2)$

$$\Psi^m(x) = \Psi^m(x=0) + c_2 x^2 + c_3 x^3 + \ldots$$

- Fit results of runs at various resolutions to this model, and extrapolate to $x = 0$

Richardson extrapolation (II)

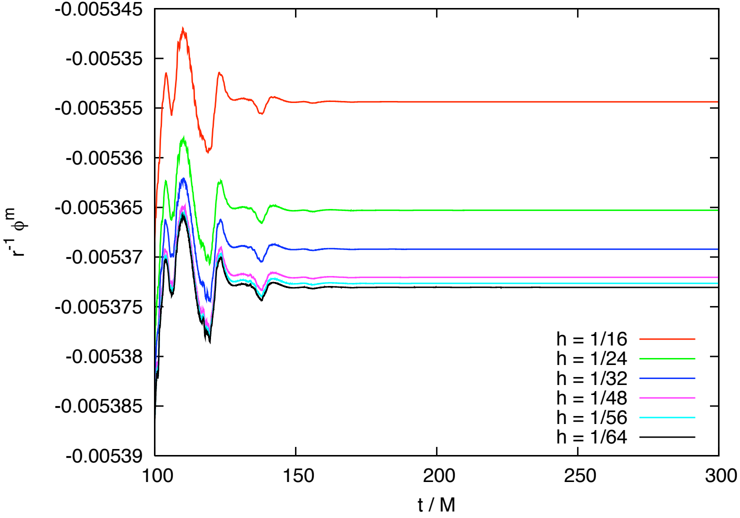

Richardson extrapolation (III)

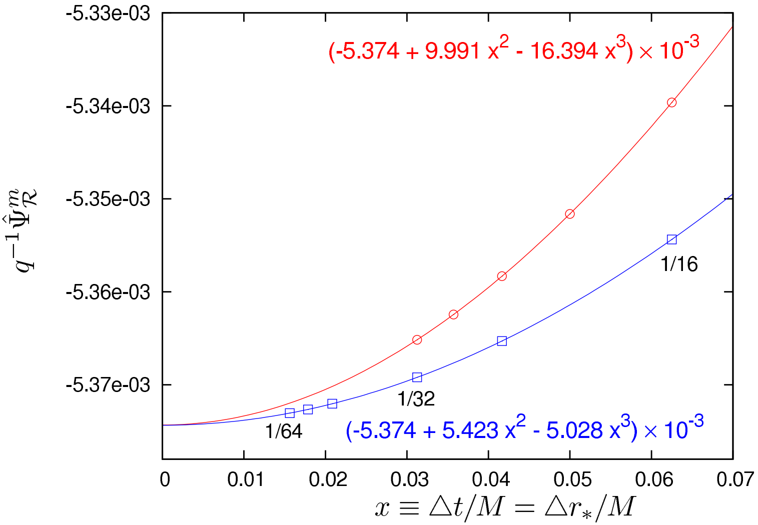

Modal convergence: F_ϕ^m

- Exponential convergence of dissipative component

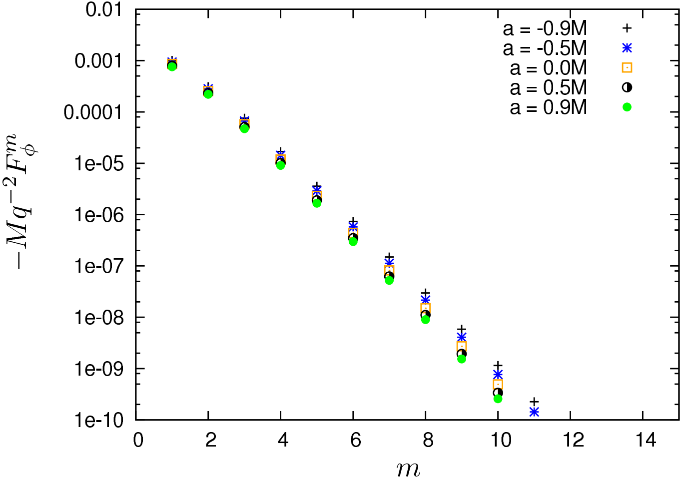

Modal convergence: F_r^m

- Power-law convergence of conservative component
- Puncture orders $n = 2$, 3 and 4

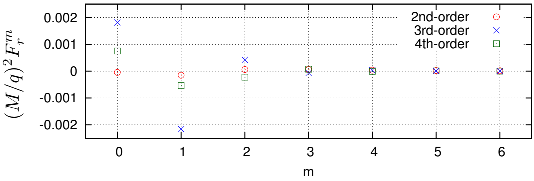

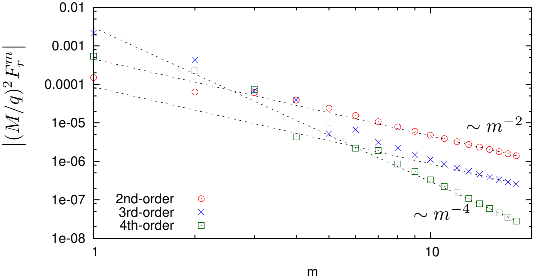

Modal convergence: F_r^m

4th-order puncture ... m^{-4} convergence

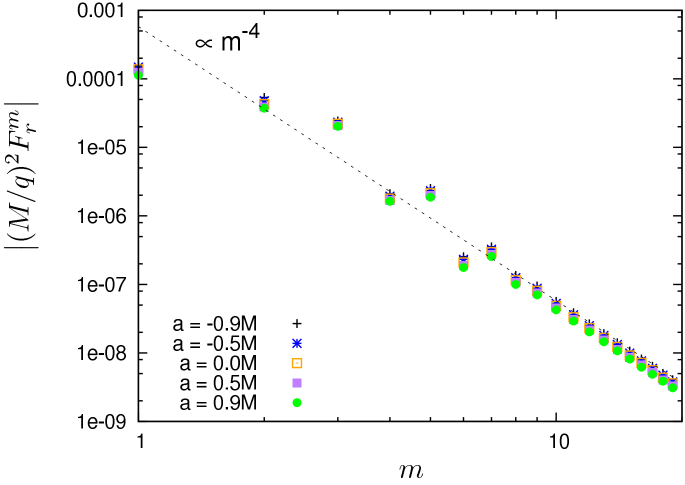

Modal convergence: F_r^m

rescaled variable $m^4 F_r^m$

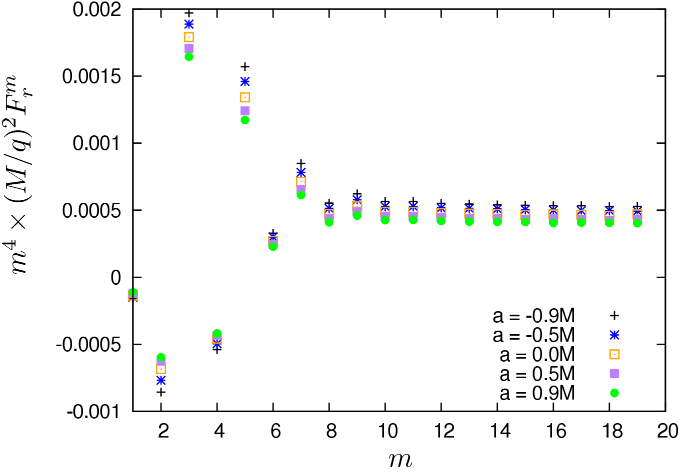

Results: scalar-field SF on Kerr

F_r for circular orbits in equatorial plane

Radial component of SF, $(M^2/q^2)F_r^{\text{self}}$			
	$r_0 = 6M$	$r_0 = 10M$	$r_0 = r_{\text{isco}}$
$a = -0.9M$	– –	4.941(1) 4.39995 $\times 10^{-5}$	9.6074(7) 9.607001 $\times 10^{-5}$
$a = -0.7M$	– –	4.102(1) 4.100712 $\times 10^{-5}$	1.1077(2) 1.107625 $\times 10^{-4}$
$a = -0.5M$	– –	3.290(1) 3.28942 $\times 10^{-5}$	1.2751(2) 1.275170 $\times 10^{-4}$
$a = \quad 0M$	1.6771(2) 1.677283 $\times 10^{-4}$	1.379(1) 1.378448 $\times 10^{-5}$	1.6771(2) 1.677283 $\times 10^{-4}$
$a = +0.5M$	−2.423(4) −2.421685 $\times 10^{-5}$	−4.028(9) −4.03517 $\times 10^{-6}$	−6.925(5) −6.922147 $\times 10^{-5}$
$a = +0.7M$	−9.530(3) −9.528095 $\times 10^{-5}$	−1.0913(9) −1.091819 $\times 10^{-5}$	−1.0886(4) −1.088457 $\times 10^{-3}$
$a = +0.9M$	−1.6458(5) −1.645525 $\times 10^{-4}$	−1.767(1) −1.768232 $\times 10^{-5}$	−1.1344(9) −1.133673 $\times 10^{-2}$

Results: scalar-field SF on Kerr

F_ϕ for circular orbits in equatorial plane

Angular component of SF, $-(M/q^2)F_\phi^{\text{self}}$			
	$r_0 = 6M$	$r_0 = 10M$	$r_0 = r_{\text{isco}}$
$a = -0.9M$	– –	1.41470(1) 1.414708 $\times 10^{-3}$	2.18835(1) 2.188351 $\times 10^{-3}$
$a = -0.7M$	– –	1.35624(1) 1.356244 $\times 10^{-3}$	2.57803(1) 2.578045 $\times 10^{-3}$
$a = -0.5M$	– –	1.30226(1) 1.302267 $\times 10^{-3}$	3.08354(1) 3.083542 $\times 10^{-3}$
$a = \quad 0M$	5.304230(3) 5.3042317 $\times 10^{-3}$	1.18592(1) 1.185926 $\times 10^{-3}$	5.30423(1) 5.304232 $\times 10^{-3}$
$a = +0.5M$	4.230745(3) 4.230749 $\times 10^{-3}$	1.09349(1) 1.093493 $\times 10^{-3}$	1.18357(4) 1.183567 $\times 10^{-2}$
$a = +0.7M$	3.928695(3) 3.928698 $\times 10^{-3}$	1.06216(1) 1.062163 $\times 10^{-3}$	1.94873(1) 1.948731 $\times 10^{-2}$
$a = +0.9M$	3.676723(8) 3.676726 $\times 10^{-3}$	1.03344(1) 1.0334444 $\times 10^{-3}$	4.5079(2) 4.508170 $\times 10^{-2}$

- So much for the scalar field ... what about the interesting case?
- Einstein equations :

$$G_{ab} \equiv R_{ab} - \frac{1}{2} g_{ab} R = 8\pi T_{ab}$$

- Vacuum background + stress-energy $T_{ab} \propto$ 'small' parameter $\mu = m/M$
- Metric split : background + perturbation :

$$g_{ab} = \hat{g}_{ab} + \mu h_{ab}$$

- Trace-reversed perturbation $\bar{h}_{ab}$:

$$\bar{h}_{ab} = h_{ab} - \frac{1}{2} g_{ab} h$$

Gravitational SF on Kerr

- Linearized equations:

$$\Delta_L \bar{h}_{ab} \equiv \nabla^c \nabla_c \bar{h}_{ab} + 2\, R^c{}_a{}^d{}_b\, \bar{h}_{cd} + g_{ab} \mathcal{Z}^c_{;c} - \mathcal{Z}_{a;b} - \mathcal{Z}_{b;a} = -16\pi T_{ab}$$

where

$$\mathcal{Z}^b \equiv \nabla_a \bar{h}^{ab}$$

- Mixed hyperbolic-elliptic type equations.
- Impose Lorenz gauge conditions $\mathcal{Z}_a = 0 \Rightarrow \Box \mathcal{Z}_a = 0$.
- How to enforce gauge conditions? Gauge-constraint damping [Gundlach *et al.* '05]

$$\nabla^c \nabla_c \bar{h}_{ab} + 2\, R^c{}_a{}^d{}_b\, \bar{h}_{cd} + n_a \mathcal{Z}_b + n_b \mathcal{Z}_a = -16\pi T_{ab}.$$

Gravitational SF on Kerr

- m-mode decomposition:

$$\bar{h}_{ab} = \alpha_{ab}(r,\theta) u_{ab}(r,\theta,t) e^{im\phi}, \qquad \text{(no sum)}$$

- 10 wave equations:

$$\Box_{sc} u_{ab} + \mathcal{M}_{ab}(u_{cd,t}, u_{cd,r_*}, u_{cd,\theta}, u_{cd}) = S_{ab}$$

2+1D Wave Equations (Schw.)

$$f\Box_{sc}u_{ab} + \mathcal{M}_{ab}(\dot{u}_{cd,t}, u_{cd,r*}, u_{cd,\theta}, u_{cd}) = 0$$

$$\begin{aligned}
\mathcal{M}_{00} &= \frac{2\left(2r^2(\dot{u}_{01} - u'_{00}) + u_{00} - u_{11}\right)}{r^4} + \frac{4f\left(u_{00} - u_{11}\right)}{r^3} + \frac{2f^2\left(u_{22} + u_{33}\right)}{r^3} \\
\mathcal{M}_{01} &= -\frac{2f^2\left(\cos\theta u_{02} + imu_{03}\right)}{r^2\sin\theta} + \frac{2(\dot{u}_{00} + \dot{u}_{11} - 2u'_{01})}{r^2} - \frac{2f^2(u_{01} + \partial_\theta u_{02})}{r^2} \\
\mathcal{M}_{02} &= -\frac{f(u_{02} + 2im\cos\theta u_{03})}{r^2\sin^2\theta} + \frac{2(\dot{u}_{12} - u'_{02})}{r^2} + \frac{f[(4+r)u_{02} + 2r\partial_\theta u_{01}]}{r^3} - \frac{f^2 u_{02}}{r^2} \\
\mathcal{M}_{03} &= -\frac{f(u_{03} - 2im\cos\theta u_{02})}{r^2\sin^2\theta} + \frac{2fimu_{01}}{r^2\sin\theta} + \frac{2(\dot{u}_{13} - u'_{03})}{r^2} + \frac{f(4+r)u_{03}}{r^3} - \frac{f^2 u_{03}}{r^2} \\
\mathcal{M}_{11} &= -\frac{4f^2(\cos\theta u_{12} + imu_{13})}{r^2\sin\theta} + \frac{2[2r^2(\dot{u}_{01} - u'_{11}) + u_{11} - u_{00}]}{r^4} - \frac{4f(u_{00} - u_{11})}{r^3} \\
&\quad -\frac{2f^2(2ru_{11} + u_{22} + u_{33} + 2r\partial_\theta u_{12})}{r^3} + \frac{2f^3(u_{22} + u_{33})}{r^2} \\
\mathcal{M}_{12} &= -\frac{f(u_{12} + 2im\cos\theta u_{13})}{r^2\sin^2\theta} - \frac{2f^2[\cos\theta(u_{22} - u_{33}) + imu_{23}]}{r^2\sin\theta} + \frac{2(\dot{u}_{02} - u'_{12})}{r^2} \\
&\quad +\frac{f[(4+r)u_{12} + 2r\partial_\theta u_{11}]}{r^3} - \frac{f^2(5u_{12} + 2\partial_\theta u_{22})}{r^2}
\end{aligned}$$

2+1D Wave Equations (Schw.)

$$f\Box_{sc}u_{ab} + \mathcal{M}_{ab}(\dot{u}_{cd,t}, u_{cd,r*}, u_{cd,\theta}, u_{cd}) = 0$$

$$\begin{aligned}
\mathcal{M}_{13} &= -\frac{f(u_{13} - 2im\cos\theta u_{12})}{r^2\sin^2\theta} - \frac{2f[2f\cos\theta u_{23} + im(fu_{33} - u_{11})]}{r^2\sin\theta} + \frac{2(\dot{u}_{03} - u'_{13})}{r^2} \\
&\quad + \frac{f(4+r)u_{13}}{r^3} - \frac{f^2(5u_{13} + 2\partial_\theta u_{23})}{r^2} \\
\mathcal{M}_{22} &= -\frac{2f[u_{22} - u_{33} + 2im\cos\theta u_{23}]}{r^2\sin^2\theta} + \frac{2(u_{00} - u_{11})}{r^3} + \frac{2f(u_{11} + u_{22} + 2\partial_\theta u_{12})}{r^2} \\
&\quad - \frac{2f^2(u_{22} + u_{33})}{r^2} \\
\mathcal{M}_{23} &= -\frac{2f[2u_{23} - im\cos\theta(u_{22} - u_{33})]}{r^2\sin^2\theta} - \frac{2f(\cos\theta u_{13} - imu_{12})}{r^2\sin\theta} + \frac{2f(u_{23} + \partial_\theta u_{13})}{r^2} \\
\mathcal{M}_{33} &= \frac{2f(u_{22} - u_{33} + 2im\cos\theta u_{23})}{r^2\sin^2\theta} + \frac{4f(\cos\theta u_{12} + imu_{13})}{r^2\sin\theta} + \frac{2(u_{00} - u_{11})}{r^3} \\
&\quad + \frac{2f(u_{11} + u_{33})}{r^2} - \frac{2f^2(u_{22} + u_{33})}{r^2}.
\end{aligned}$$

Gauge constraint damping

- Imperfect, gauge-violating initial data

$$\Rightarrow \mathcal{Z}^a \equiv \nabla_b \bar{h}^{ab} \neq 0.$$

- Gauge-violation itself obeys a wave equation:

$$\Box \mathcal{Z}^a = 0.$$

- How to drive system towards Lorenz gauge solution $\mathcal{Z}^a = 0$?
- Gauge Constraint Damping: add extra term to wave equations featuring gauge violation vector $\mathcal{Z}_a$, i.e.

$$\Box \bar{h}_{ab} + 2R^c{}_a{}^d{}_b \bar{h}_{cd} + (n_a \mathcal{Z}_b + n_b \mathcal{Z}_a) = 0.$$

so that $\mathcal{Z}_a$ obeys a damped wave equation

2nd-order puncture scheme

- Barack, Golbourn & Sago (2007) give a 2nd-order puncture formulation:

$$\bar{h}^P_{ab}(x) = \frac{\mu}{\epsilon_P^{[2]}} \chi_{ab}, \qquad \chi_{ab} = \left[u_a u_b + (\Gamma^c_{ad} u_b + \Gamma^c_{bd} u_a) u_c \delta x^d \right]_{x=\bar{x}}$$

- For circular orbits in equatorial plane, this reduces to

$$\begin{aligned}
\chi_{00} &= C_{00} + D_{00}\delta r \\
\chi_{01} &= D_{01} \sin \delta\phi \\
\chi_{03} &= C_{03} + D_{03}\delta r \\
\chi_{13} &= D_{13} \sin \delta\phi \\
\chi_{33} &= C_{33} + D_{33}\delta r
\end{aligned}$$

2nd-order puncture scheme

- Effective source: $S^{\text{eff}}_{ab} = \Box \bar{h}^P_{ab} + 2R^c{}_a{}^d{}_b \bar{h}^P_{cd}$
- m-mode decomposition: $\bar{h}^{P(m)}_{ab}$ and $S^{\text{eff}(m)}_{ab}$
- Puncture and source found in terms of 'symmetric' elliptic integrals $I^m_1, \ldots, I^m_5$ ...
- ... and antisymmetric integrals $J^m_1, \ldots, J^m_5$ ...

$$\begin{aligned}
\int_{-\pi}^{\pi} \epsilon_P^{-3} \sin\delta\phi \, e^{-im\delta\phi} d(\delta\phi) &= \frac{-i}{B^{3/2}\rho} \left[q^m_{1K} K(i/\rho) + \rho^2 q^m_{1E} E(i/\rho) \right] \\
\int_{-\pi}^{\pi} \epsilon_P^{-3} \sin\delta\phi \, \cos\delta\phi \, e^{-im\delta\phi} d(\delta\phi) &= \frac{-i\gamma}{B^{3/2}} \left[q^m_{2K} K(\gamma) + q^m_{2E} E(\gamma) \right] \\
\int_{-\pi}^{\pi} \epsilon_P^{-5} \sin\delta\phi \, \cos^2(\delta\phi/2) \, e^{-im\delta\phi} d(\delta\phi) &= \frac{-i\gamma}{B^{5/2}} \left[q^m_{3K} K(\gamma) + \rho^{-2} q^m_{3E} E(\gamma) \right] \\
\int_{-\pi}^{\pi} \epsilon_P^{-5} \sin\delta\phi \, \sin^2(\delta\phi) \, e^{-im\delta\phi} d(\delta\phi) &= \frac{-i}{B^{5/2}\rho} \left[q^m_{4K} K(i/\rho) + \rho^2 q^m_{4E} E(i/\rho) \right] \\
\int_{-\pi}^{\pi} \epsilon_P^{-5} \sin\delta\phi \, \sin^2(\delta\phi/2) \, e^{-im\delta\phi} d(\delta\phi) &= \frac{-i\gamma^2}{B^{5/2}\rho} \left[q^m_{5K} K(i/\rho) + \rho^2 q^m_{5E} E(i/\rho) \right]
\end{aligned}$$

- Wardell and co. developing a 4th-order scheme

Metric Perturbations : Time evolution

Regularized field at particle in circular orbit: $r_0 = 7M$, $m = 2$

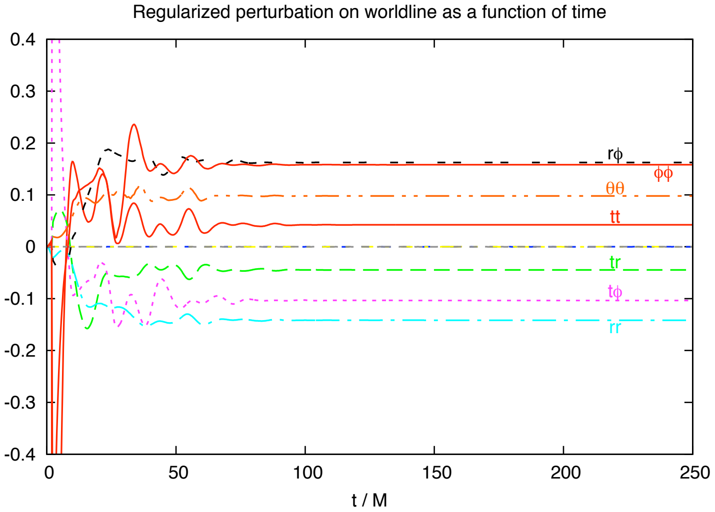

Gauge Violation : Time evolution

$r_0 = 7M$, $m = 2$

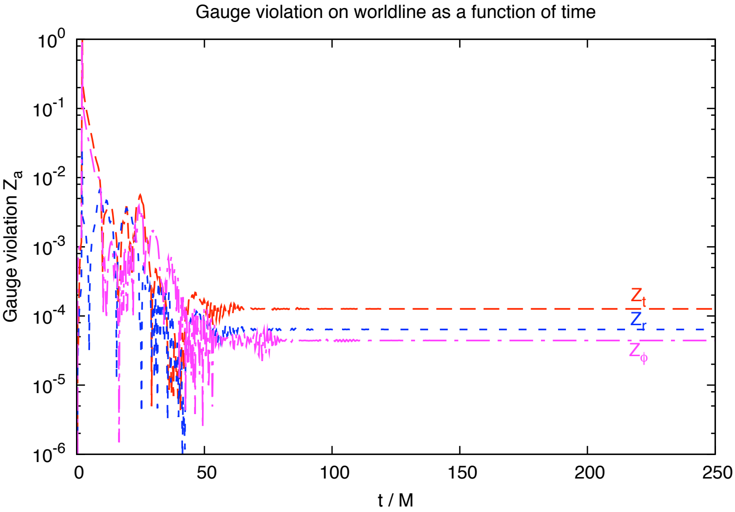

Metric Perturbations : Angular Profile

$r_0 = 7M$, $m = 2$

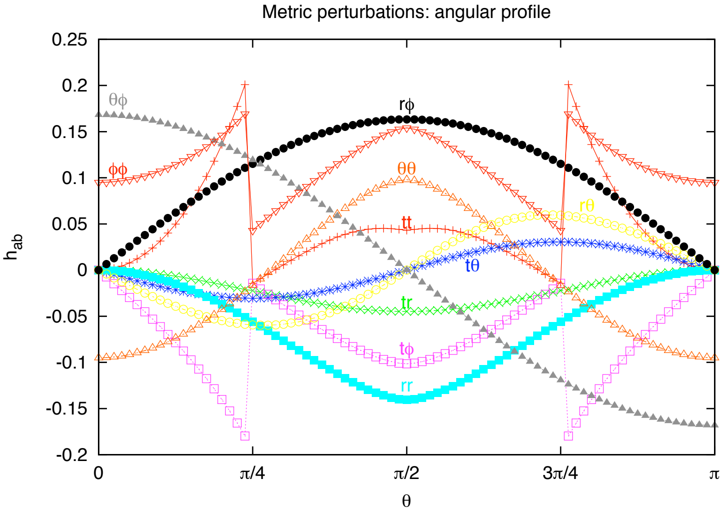

Metric Perturbations : Angular Profile

$r_0 = 7M$, $m = 2$

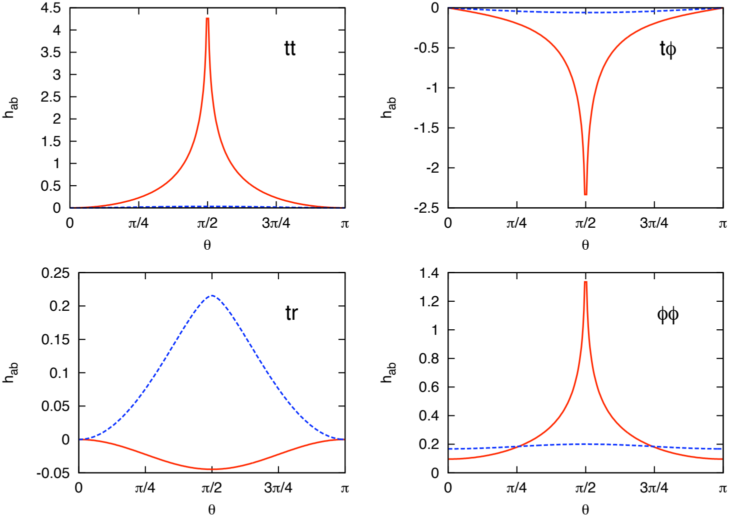

l-mode and m-modes

- Project out: m-modes $u^m_{ab}(t, r, \theta)$ onto lm modes $h^{(i)}_{lm}(t, r)$ of Barack/Lousto/Sago.
- Use tensor spherical harmonics $i = 1 \ldots 10$,

$$h^{(1)}_{lm}(r,t) = 2\pi \int_0^\pi \sin x \, (u_{00} + u_{11}) \, Y^*_{lm}(x) dx \quad (3)$$

$$h^{(2)}_{lm}(r,t) = 2\pi \int_0^\pi \sin x \, 2u_{01} Y^*_{lm}(x) dx \quad (4)$$

$$h^{(3)}_{lm}(r,t) = 2\pi \int_0^\pi \sin x \, (u_{00} - u_{11}) \, Y^*_{lm}(x) dx \quad (5)$$

$$h^{(4)}_{lm}(r,t) = 4\pi \int_0^\pi [\sin x \, u_{02} \, \partial_x - imu_{03}] \, Y^*_{lm} dx \quad (6)$$

$$h^{(5)}_{lm}(r,t) = 4\pi \int_0^\pi [\sin x \, u_{12} \, \partial_x - imu_{13}] \, Y^*_{lm} dx \quad (7)$$

$$h^{(6)}_{lm}(r,t) = 2\pi \int_0^\pi \sin x \, (u_{22} + u_{33}) \, Y^*_{lm} dx \quad (8)$$

$$h^{(7)}_{lm}(r,t) = 2\pi \int_0^\pi [\sin x (u_{22} - u_{33}) D_2 + 2u_{23} D_1] \, Y^*_{lm} dx \quad (9)$$

Comparison with l-modes

Projection from m modes onto lm modes of Barack/Lousto/Sago

	$l = 2,\ m = 2$	
$i = 1$	3.1246	$-0.2630i$
	3.1246	$-0.2632i$
$i = 2$	-0.2316	$0.9755i$
	-0.2312	$0.9758i$
$i = 3$	5.3159	$0.6164i$
	5.3162	$0.6162i$
$i = 4$	-0.9269	$9.4275i$
	-0.9249	$9.4292i$
$i = 5$	-2.3297	$-2.5279i$
	-2.3310	$-2.5279i$
$i = 6$	1.5471	$0.6009i$
	1.5468	$0.6006i$
$i = 7$	-5.3326	$-5.2205i$
	-5.3319	$-5.2190i$

Problem: Time Evolution of $m = 0$ mode

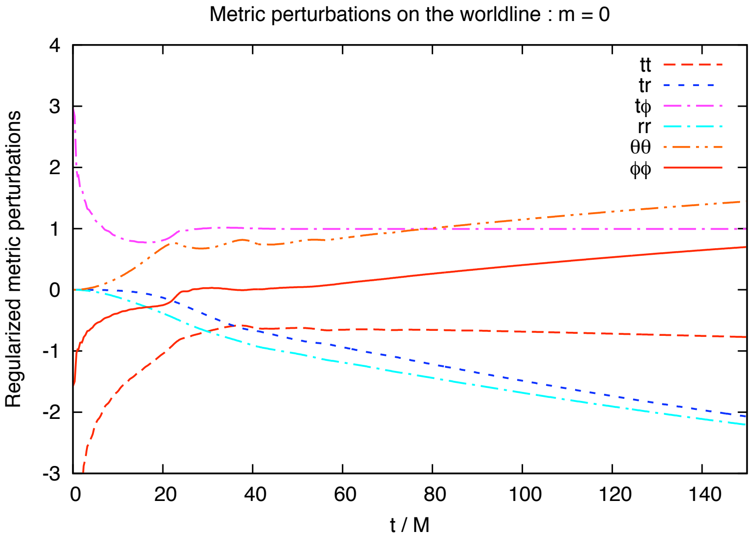

Radial Profile : $m = 0$ mode

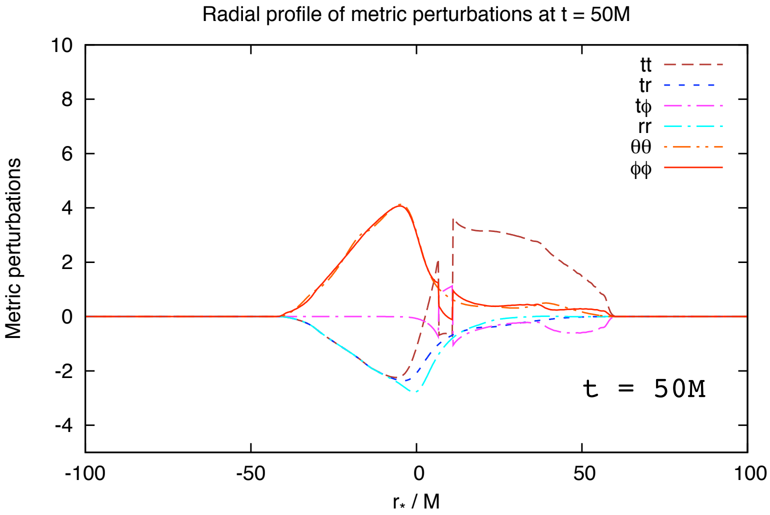

Radial Profile : $m = 0$ mode

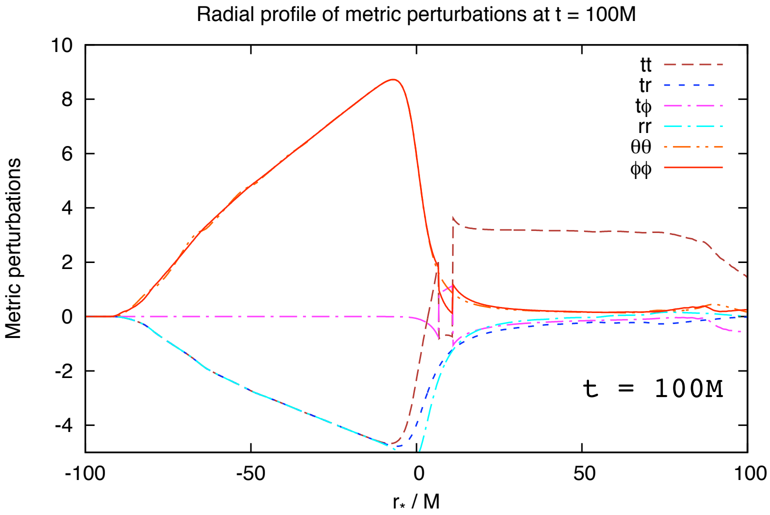

Radial Profile : $m = 0$ mode

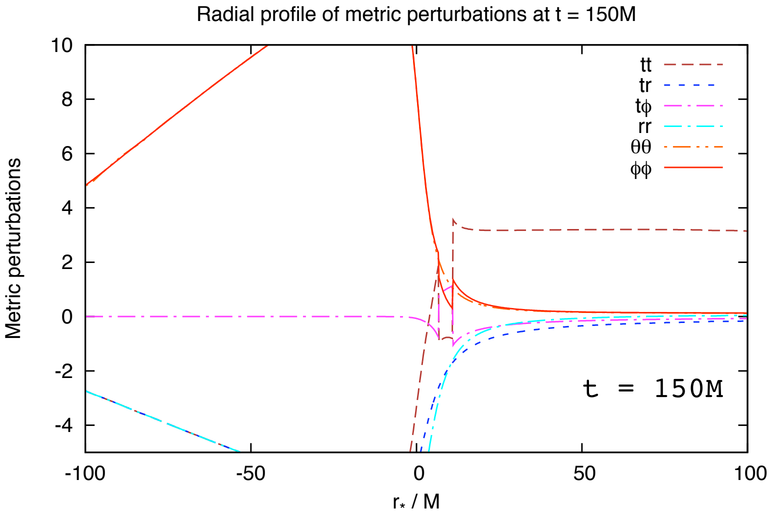

The low multipoles stability problem

- The growing solutions arise even for vacuum perturbations.
- The growing solutions are (locally) Lorenz-gauge
- They are homogeneous and pure-gauge: $h_{ab} = \xi_{a;b} + \xi_{b;a}$
- They are 'scalar' gauge modes: $\xi_a = \Phi_{;a}$.
- The growing solutions satisfy ingoing conditions at horizon:

$$u \sim t + 2\ln(1 - 2/r) \qquad \Rightarrow \qquad \left(\frac{\partial}{\partial t} - \frac{\partial}{\partial r_*}\right) u = 0$$

- The growing solutions are traceless $h = -\bar{h}^a_a = 0$.
- The problem is entirely in $l = m = 0$ and $l = m = 1$ modes.
- Q. Why has no-one evolved Schw. $l = 0$ and $l = 1$ modes in time-domain?
- A. Negative potentials $(r < 3M)$, unstable evolutions.

Lorenz-Gauge Monopole Modes

- Pure-gauge modes generated by gauge vectors ξ_a

$$h_{ab} = \xi_{(a;b)} \quad \Rightarrow \quad \bar{h}_{ab} = \xi_{(a;b)} - \frac{1}{2} g_{ab} \xi^{c}_{;c}$$

- Lorenz-gauge $\bar{h}^{;b}_{ab} = 0 \Rightarrow \xi_{a;b}{}^{b} = 0$
- Two scalar monopole gauge modes $\xi_a = \Phi_{;a} \Rightarrow (\Box\Phi)_{;a} = 0 \Rightarrow \Box\Phi = \{0, \text{const.}\}$
- Trace : $h = \xi^{a}_{;a} = \Box\Phi = \{0, \text{const}\}$
  $\Rightarrow$ Trace-free, static scalar gauge mode $\Phi_0 = \frac{1}{2} \ln f$
- Pseudo-static mode $\Phi = t \times \Phi_0 = \frac{t}{2} \ln f$, $\Box\Phi = 0$,

$$u_{00}, u_{11}, u_{22} \propto t, \qquad u_{01} \neq 0.$$

Pseudo-static modes

- Pseudo-static (i.e. linearly-growing) locally Lorenz-gauge modes in monopole
- How do they arise in time domain?
- To see, use conservation laws (due to symmetries of Ricci-flat background) to reduce degrees of freedom.
- Monopole: Four coupled 2nd order equations + two gauge constraints + one conservation equation.
- After reducing degrees of freedom, find wave equation with negative potential.

Conserved quantities in non-radiative multipoles (I)

- Symmetries: Background spacetime has Killing vectors X_a :

$$\nabla_a X_b + \nabla_b X_a = 0$$

- Stress-energy is conserved, $\nabla_a T^{ab} = 0$, so we can construct a conserved vector:

$$j^a \equiv T^{ab} X_b \quad \Rightarrow \quad \nabla_a j^a = 0.$$

- The vector $j_a = (-16\pi)^{-1} \mathcal{W}_{ab} X^b$ can be written

$$j^a = \nabla_b F^{ab}, \qquad \text{where} \quad F_{ab} = -F_{ba}$$

- i.e. the divergence of an antisymmetric tensor F^{ab} where

$$\boxed{(-16\pi) F_{ab} = \bar{h}_{ac;b} X^c - \bar{h}_{bc;a} X^c - \bar{h}_{ac} X^c{}_{;b} + \bar{h}_{bc} X^c{}_{;a}}$$

- Apply Stokes' theorem $\Rightarrow$ Conserved integrals on two-surfaces

Conserved quantities in non-radiative multipoles (II)

- Gauss's theorem:

$$\int_{\Sigma_1} j^a d\Sigma_a = \int_{\Sigma_2} j^a d\Sigma_a$$

- Stokes' theorem ($j^a = F^{ab}{}_{;b}$):

$$\int_{\Sigma} F^{ab}{}_{;b} d\Sigma_a = \frac{1}{2}\int_{\partial\Sigma} F^{ab} dS_{ab}$$

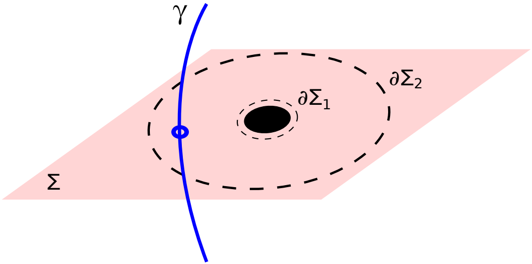

Conservation Law (III)

- Integrate on constant-t hypersurfaces, on concentric spheres:
- $X_a^{(t)} \Rightarrow$ Energy $\mathcal{E}$, $\quad X_a^{(\phi)} \Rightarrow$ Ang. Mom. $\mathcal{L}_z$ in perturbation
- Ang. mom. in $l = 1$ odd-parity sector, energy is in monopole ($l = 0$),

$$4\pi \left[r^2 F_{01}^{(t)} \right]_{r_1}^{r_2} = \begin{cases} \mathcal{E} \equiv -u_t, & r_1 < r_0 < r_2, \\ 0, & \text{otherwise.} \end{cases}$$

- Locally conserved quantity in monopole ($l = m = 0$) equations:

$$r^2 \left(\bar{h}_{tt,r} - \bar{h}_{tr,t} \right) - 2f^{-1}\bar{h}_{tt} + 2f\bar{h}_{rr} = \begin{cases} -4\mathcal{E}, & r > r_0, \\ 0, & r < r_0. \end{cases}$$

Monopole equations

- Monopole has four equations $(u_{00}, u_{01}, u_{11}, u_{22} = u_{33})$ + two gauge constraints.
- Trace equation evolve stably
- Use conserved quantity $C = \begin{cases} -4\mathcal{E} & r < r_0 \\ 0 & r > r_0 \end{cases}$
- Hierarchical system of equations for $\{H, X, Y\}$

$$\begin{aligned} D^2 H &= 0 \\ D^2 X &= \frac{2f}{r^4} H - \frac{3fC}{r^3} \\ \left[D^2 - \frac{2f}{r^2}\left(1 - \frac{4M}{r}\right)\right] Y &= -\frac{4f}{r^2} H + \frac{2f}{r} C \end{aligned}$$

where $D^2 = -\partial_t^2 + \partial_{r^*}^2 - 2fM/r^3$

- $H = r\bar{h}^a_a$, $X = (2rf)^{-1}\left[u_{11} - (2r-3)u_{00}\right]$, $Y = rf^{-1}(u_{00} - u_{11})$.

Monopole equations

- H and X equations evolve stably. Y equation does not.
- Y equation resembles a Regge-Wheeler equation

$$\left[-\frac{\partial^2}{\partial t^2} + \frac{\partial^2}{\partial r_*^2} - V_{12}(r)\right] Y = \dots$$

where

$$V_{ls}(r) = f\left(\frac{l(l+1)}{r^2} - \frac{2M(1-s^2)}{r^3}\right)$$

i.e. here $l = 1, \, s = 2$.

- Potential turns negative within $r < 3M \Rightarrow$ growing modes.
- In principle, Y can be recovered from H, X by integrating conservation law on spatial slices:

$$\frac{\partial}{\partial r^*}(rY) = r[C - 2X - fH].$$

Challenges for time-domain Lorenz gauge formulation

- How do we evolve $l = 0$, $l = 1$ modes in time domain in 1+1D?
- e.g. how do we eliminate trace-free, massless, locally-Lorenz gauge modes? (in monopole and dipole)
- How do we enforce the physical boundary condition at the horizon?

Ideas . . . :

1. Use of generalized Lorenz gauge to promote stability,

$$\bar{h}_{\mu\nu}^{;\nu} = H_\mu(\bar{h}_{\alpha\beta}; r).$$

2. Horizon-penetrating coordinates? (e.g. ingoing Eddington-Fink.). Hyperboloidal slicing?
3. Restricted set of variables, with reconstruction of metric by integrating first-order conservation equations?

Generalized Lorenz gauge

- I have tried a generalized Lorenz gauge (GLG) of the form
$$\bar{h}_{ab}^{;b} = H_a(h_{tr})$$
- For circular orbits, we want the monopole part of h_{tr} to be zero.
- I can achieve stable evolutions if I make H_a proportional to an ingoing null vector.
- With analytically-known $l = 0, m = 0$ monopole as initial data, the 2+1D scheme evolves stably with $h_{tr} \to 0$ as grid spacing $\to 0$.
- I have not yet found a GLG which stabilizes the $m = 1, l = 1$ even-parity dipole ...
- ... but since the undesirable mode grows linearly (whereas physical part $\sim \exp(im\Omega t)$), I can eliminate it:
$$h \to -\frac{1}{\Omega^2}\frac{\partial^2}{\partial t^2}h$$

Recent progress

- These ‘tricks’ now make it possible to compute Lorenz-gauge GSF for circular orbits, using 2+1D approach.
- With a second-order puncture, and max. resolution $\Delta r_* = M/16$, I can compute F_r to accuracy greater than 0.05%, for $r_0 = 6M$ on Schw.
- I have written the first Lorenz-gauge 2+1D Kerr code.
- To validate, may compare F_t against the energy fluxes computed via the Teukolsky formalism

Recent progress: Dissipative GSF in Kerr

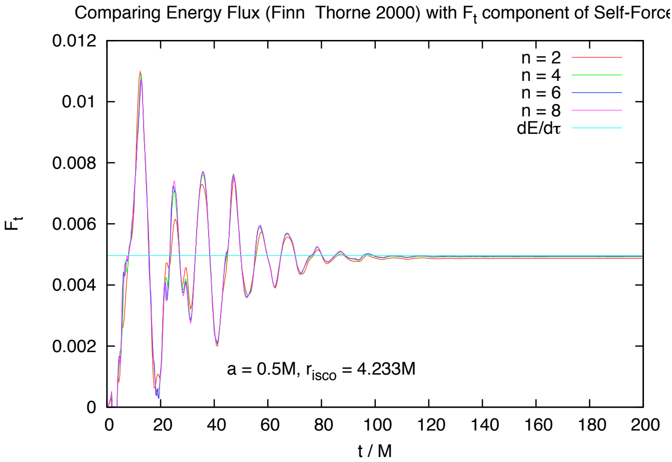

- $m = 2$ mode (radiative)
- Showing results of various grid resolutions $x \equiv M/n$.

Recent progress: Dissipative GSF in Kerr

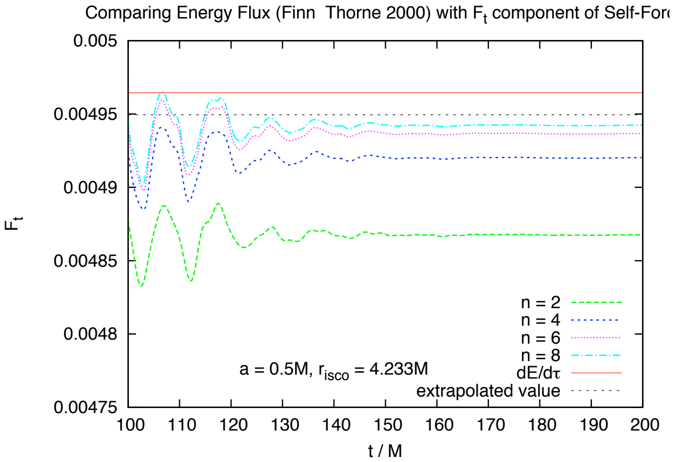

- 2nd-order puncture $\Rightarrow S \sim \ln(|r - r_0|) \Rightarrow x^2 \ln x$ convergence.
- 0.4% here error still unexplained ...

Summary of progress: m-mode $2+1$D method

- Scalar field, first-order puncture: Barack & Golbourn [arXiv:0705.3620].
- Second-order GSF formulation: Barack, Golbourn & Sago [arXiv:0709.4588].
- Scalar-field, fourth-order punc, Schw.: Dolan & Barack [arXiv:1010.5255]
- Scalar-field, Kerr, circ orbits: Dolan, Wardell & Barack [arXiv:1107.0012]
- Scalar-field, Kerr, eccentric orbits: Thornburg (in progress)
- GSF, Schw, circ. orbits, 2nd order: Dolan & Barack (in progress)
- GSF, Kerr, circ. orbits, 4th order: coming soon (I hope!).

Summary

- GSF programme for black hole inspirals recently came-of-age (in 2009) with comparison of physically-meaningful numerical results on Schwarzschild with other methodologies.
- First comparisons of GSF with PN, EOB and NR have been successful.
- First 'self-forced' orbits and waveforms produced recently (Gair *et al.*)
- Very interesting resonance phenomenon (Hinderer & Flanagan) expected for EMRIs on Kerr. Details require Kerr GSF.
- First GSF calculations on Kerr underway (Dolan 2011; Friedman 2011).
- Second-order formalism is under discussion; numerical work someway off.
- Lots of interesting calculations still to do!